Structural, Morphological and Spectral Properties of $La_2Mo_2O_9$ Thin Films Synthesized by Spray Pyrolysis Technique

G. A. Kadam[1], S. A. Patil[2], B. B. Patil[3], L. D. Kadam[4], R. K. Nimat[1*]

[1]*Department of Physics, Balasaheb Desai College, Patan, Maharashtra, India 415206.*
[2]*Department of Physics, D. Y. Patil Medical College, Kolhapur, Maharashtra, India 416006.*
[2]*Department of Physics, KRP Kanya Mahavidyalaya, Islampur, Maharashtra, India 415409.*
[1]*Department of Physics, Dr. Patangrao Kadam Mahavidyalaya, Burli, Maharashtra, India 416308.*

Abstract: *The $La_2Mo_2O_9$ (LAMOX) thin films were prepared successfully by using chemical spray pyrolysis method and annealed at 1000 ℃ for two hours. LAMOX thin films were characterized by XRD, FESEM and EDAX tools. X-ray diffraction result shows the increase in crystallite size with deposition temperature LAMOX thin film. The morphological investigation were done by analyzing FESEM. It is shows that, increase in grain size after the annealing. The investigated LAMOX are potential application as an electrolyte for solid oxide fuel cell.*

Keywords: LAMOX, XRD, FESEM, EDAX.

*corresponding author
Dr. R. K. Nimat
Associate Professor,
Balasaheb Desai College, Patan
Tal.- Patan, Dist.- Satara
Maharashtra, India 415206

1. Introduction

From the discovery of $La_2Mo_2O_9$ (LAMOX) material, it plays a crucial role in the application of solid oxide fuel cell (SOFC) as an electrolyte because of its oxide ion conductivity at intermediate temperature [1-3]. La^{3+} based compounds also shows beneficial parameters for SOFC applications [4, 5]. The most important factor affecting on the performance of electrolyte is their oxygen ion conductivity. Before the discovery of LAMOX the YSZ (Yttria Stabilized Zirconia) used as electrolyte having good ionic conductivity 0.1 S cm^{-1} at 1000 ℃ [6]. YSZ necessitates not only costly interconnects but also contributes into cell ohmic loss, raising the cost of fuel cells. Lacorre et al. [7] discovered LAMOX family of oxygen ion conductors in the 2000. The function of LAMOX is based on concept of lone pair substitution (LPS) [8].

At intermediate temperatures, LAMOX has higher oxygen ion conduction ability than YSZ [7]. Fournier et al. synthesized the first $La_2Mo_2O_9$ compound in 1970. At around 580 ℃, the compound phase transition from monoclinic to cubic phase [9, 10]. Fast oxide-ion conductors, has their potential applications in SOFC, oxygen sensors, and oxygen pumping devices [11-15]. The phase transition of LAMOX takes place near about 580 ℃ from α-monoclinic to β-cubic phase with enhancing ionic conductivity of order twice magnitude leading high ionic conductivity than YSZ. The ionic conductivity of electrolyte can be also enhanced by reducing the thickness of electrolyte or by discovering another type of electrolyte having high oxide ion conduction ability. Therefor the LAMOX reported as another fast oxide ion conductor used as an electrolyte material for solid oxide fuel cell [16].

2. Experimental

2.1. Synthesis of LAMOX thin films

The spray pyrolysis route was employed to deposit LAMOX thin films on an alumina (Al_2O_3) and glass substrates. The following analytical grade chemicals were directly used for the synthesis of $La_2Mo_2O_9$ (LAMOX) thin films without any further

treatment. Lanthanum chloride ($LaCl_3$ $7H_2O$) and molybdic acid (MoO_3 H_2O) were used as a precursor with a proper molar concentration ratio for the synthesis of LAMOX thin films. The solubility of the lanthanum chloride and molybdic acid salts having weights 957 g/L and 1.51 g/L in double distilled water at room temperature (25 ℃). Due to major difference in solubility factor, the solutions of lanthanum chloride and molybdic acid precursors were separately prepared. The solution of lanthanum chloride was prepared by dissolving a specific amount of lanthanum chloride in required amount of double distilled water. On the other hand, molybdic acid initially dissolved with a specific amount of concentrated HNO_3 under vigorous stirring for 15 min at room temperature. The specific amount of water was poured drop-wise to get a clear and transparent solution with continuous stirring up to 15 min. Further, both the solutions were mixed together by maintaining molar ratio as 1:1. The final combined aqueous solution of lanthanum chloride and molybdic acid used for further synthesis of LAMOX thin using chemical spray pyrolysis method.

2.2. Characterizations

The crystal structure of LAMOX thin films were decided by mini flex X-ray diffractometer with Cu-K_α radiation (λ = 1.540 Å). The morphological study of LAMOX thin films were investigated using field emission scanning electron microscopy (FESEM, JEOL JSM-6500F). EDAX (Energy dispersive X-ray spectroscopy) Oxford instruments model ASTM E1508-98 was used to investigate the elemental composition with atomic and weight % of deposited LAMOX thin films. Fourier transform infrared spectroscopy analysis of LAMOX thin were carried out by FTIR (model Lambda-7600) within the wavenumber range from 400 cm^{-1} to 4000 cm^{-1}.

3. Result and discussion

3.1 X-ray Diffraction (XRD)

XRD pattern of deposited LAMOX thin films on alumina substrate at different temperatures are displayed in fig. 1. The reflection peaks (200), (210), (211), (221), (311), (123), (410), (420), (430), (531) and (511) matched with corresponding peaks in JCPDS card no. 01-070-3587 confirms the formation of material. The variation in peaks intensity was observed with temperature. The splitting in characteristic peak (311) was observed between the 40.8° to 42°. The multiple small peaks at higher angles give evidence of the monoclinic structure of LAMOX. The room temperature XRD data matched well with reported by Goutenoire et al. [17]. The calculated crystallite size for the most intense peak (420) is listed in Table 1.

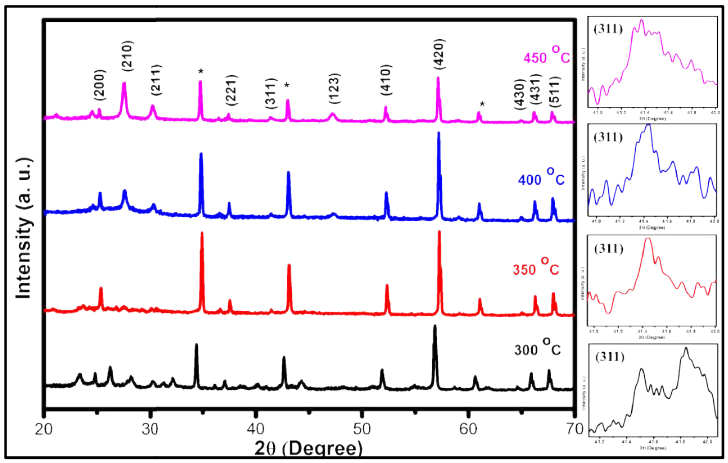

Figure 1. LAMOX XRD pattern of thin films deposited at 300 ℃, 350 ℃, 400 ℃ and 450 ℃.

Table 1. Lattice parameter, crystallite size, lattice volume, and peak intensity of LAMOX thin films.

Deposition Temp. (℃)	Lattice parameter (A°)			Crystallite Size (420) peak D (nm)	Volume V $(A°)^3$	(420) peak intensity I (a. u.)
	a	b	c			
300	7.117	7.762	6.773	52.91	374.76	199
350	7.480	6.431	7.287	73.98	350.53	400
400	7.252	6.989	7.653	74.04	387.93	1491
450	7.250	6.991	7.654	74.04	387.94	507

The fig. 2 depicted XRD pattern of annealed LAMOX thin film at 1000 ℃ for two hours. The reflection peaks at (200), (210), (211), (221), (311), (123), (410), (420), (421), (430), (431) and (511) matches with the JCPDS card number 01-070-3587 [18, 19]. The effect of annealing is noticed with variation observed in intensity of peaks, causes the change in crystallite size of LAMOX. From this study, it revealed that 400 ℃ is the optimized deposition temperature for the synthesis of LAMOX thin film. The lattice parameter and crystallite size of annealed LAMOX thin films at 1000 ℃ for two hours are depicted in below Table 2. The last compound was initially reported to crystallize in cubic symmetry with the cell lattice parameter 7.155A° [20]. The similar type of structural study of co-precipitationaly synthesized LAMOX material was carried out by Khaled et al. [21] and they observed the pre-annealed LAMOX shows α-monoclinic structure whereas annealed LAMOX shows β-cubic structure.

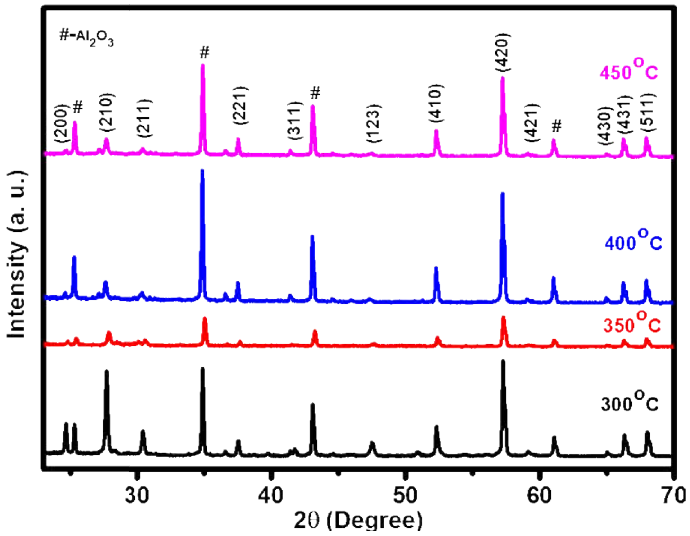

Figure 2. XRD pattern of annealed LAMOX thin film at 1000 °C.

Table 2 Lattice parameter and crystallite size of annealed LAMOX thin films.

Deposition temperature (℃)	Lattice parameter a = b = c (A°)	Crystallite size D (nm)	Cell volume V $(A°)^3$	Intensity of peak (420)
300	7.035	50.55	348.17	722
350	7.182	50.60	370.45	216
400	7.182	73.99	370.45	1708
450	7.182	73.99	370.45	1108

3.3 Field Emission Scanning Electron Microscopy (FESEM)

FESEM of deposited LAMOX thin films at constant concentration of 0.1 M at 300 ℃, 350 ℃, 400 ℃ and 450 ℃ temperatures are show in fig. 4. In spray pyrolysis method, solution droplets impending on the preheated substrate followed by ensuing process of the nucleation and growth. This complete deposition process has been described to be a function of substrate temperature [22, 23]. The fig. 3 (a) illustrates FESEM micrographs of LAMOX thin film deposited at 300 ℃, shows the porous morphology. An increase in temperature at 350 ℃ shows a slight decrease in porosity because partial evaporation of solvent takes place during the deposition shown in fig. 3 (b). The micrographs at 400 ℃ gives a more compact morphology for LAMOX thin film as shown in fig. 3 (c), which depicts compact morphology with small pours at the grain boundary. The grain size observed nearly about 0.5 µm. further increase in deposition temperature up to 450 ℃ (Fig. 3 (d)). This causes evaporation of solvent before reaching the substrate hence increasing the porosity [24].

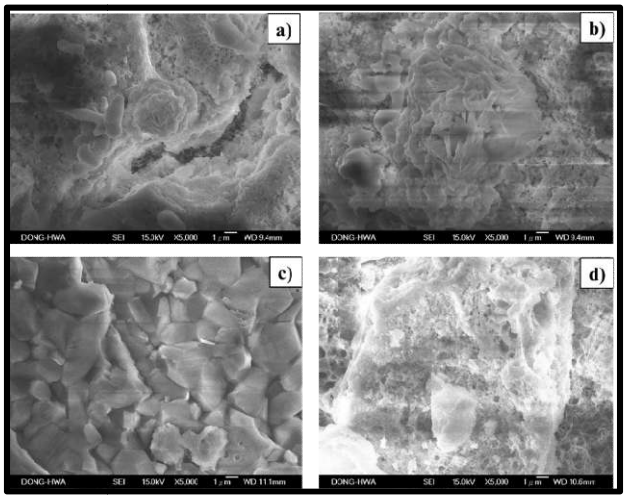

Figure 3. FESEM images of LAMOX films deposited at (a) 300 ℃ b) 350 ℃ (c) 400 ℃ (d) 450 ℃.

Morphology of annealed LAMOX thin films at 1000 ℃ for 2 h is shown in fig. 4, where most of the grain growth phenomenon has occurred due to irregular process of grain growth, where some grains grow rapidly in comparison with other grains [25]. From this figure it is quite observed that the coarsening mechanism dominates the densification and grain growth. Generally, in coarsening mechanism increases with pore size. This may be attributed to reduction in driving force and increasing diffusion distance.

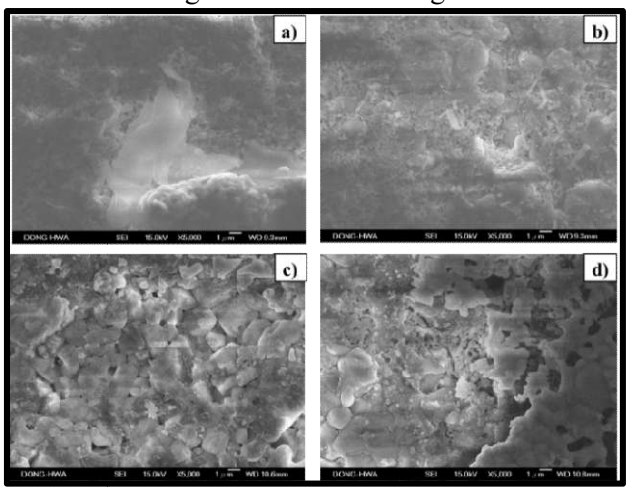

Figure 4. FESEM images of LAMOX films deposited at (a) 300 °C (b) 350 °C (c) 400 °C d) 450 °C and annealed at 1000 °C.

Optimized deposition temperature for the LAMOX thin film is 400 ℃, the porous but sufficiently dense morphology observed which is essential for the oxide ion conduction for solid oxide fuel cell.

3.4 Energy Dispersive X-ray Analysis (EDAX)

The elemental analysis of LAMOX thin film deposited at 400 °C on alumina substrate and annealed at 1000 ℃ for 2 hours revealed in fig. 5. The EDAX analysis gives the eventual proof for the presence of La, Mo, and O metal elements in LAMOX thin film.

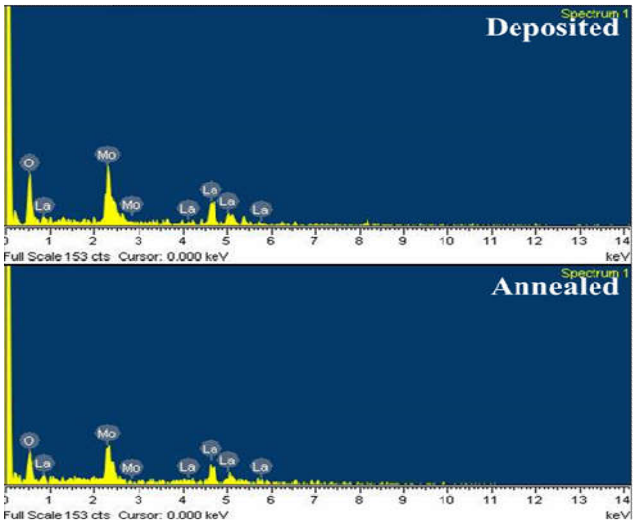

Figure 5. EDX analysis of LAMOX thin film.

The ratio of Lanthanum and Molybdenum precursor with 1:1 proportion were used for the synthesis of LAMOX thin film. From the EDAX spectra, observed atomic percentage ratio of La: Mo for deposited LAMOX thin film is 1:1.01, and weight percentage ratio is 1.3:1. For the annealed LAMOX thin film EDAX analysis shows La, Mo, and O elements. The annealing treatment effect on the weight and atomic ratio causes a decrease in individual weight percentage and increase in atomic ratio compared to the pre-annealed condition. The weight and atomic percentage of La and Mo approximately stoichiometric with required proportion. The atomic and weight percentage ration for deposited and annealed LAMOX thin film are listed in Table 3.

Table 3. The elemental composition of the LAMOX thin film.

Element	Deposited		Annealed	
	Weight %	Atomic %	Weight %	Atomic %
La	0.82	12.45	0.63	13.13
Mo	0.63	12.65	0.55	14.09
O	0.57	107.59	0.39	110.78

3.6 Fourier Transform Infrared Spectroscopy (FT-IR)

Fig.6 shows FT-IR spectra of LAMOX powder mixture with KBr scratched from pre-annealed and annealed (1000 °C for two hours) alumina substrates. The present absorption peak corresponds to 843 cm^{-1} is assigned for La-O [26]. The smaller absorption peaks at 941 cm^{-1} and 1026 cm^{-1} confirms the presence of Mo (IV)-O [27]. Within the range of 1200 to 1700 cm^{-1}, peaks at 1385 cm^{-1} and 1641 cm^{-1} are allocated for bending of NO_3^- [28]. The broad peak at 3425 cm^{-1}assigned to O-H stretching. The peaks in range of 3500 cm^{-1} to 4000 cm^{-1} assigned to presence of moisture respectively [29].

After the annealing treatment, the change in peak intensity is shows in Fig.7 (b). The broad absorption peak observed at 679 cm^{-1} is may be attributed to crystallization. The peak was observed at 2365 cm^{-1} consigned to the C-O stretching. The peak corresponding to 3425.13 cm^{-1} assigned strong stretching of O-H than the pre-annealed condition. After the 3500 cm^{-1} curves become smooth compared with pre-annealed condition, which indicates the removal of moisture from the material at 1000 ℃ and the pure phase of LAMOX is formed.

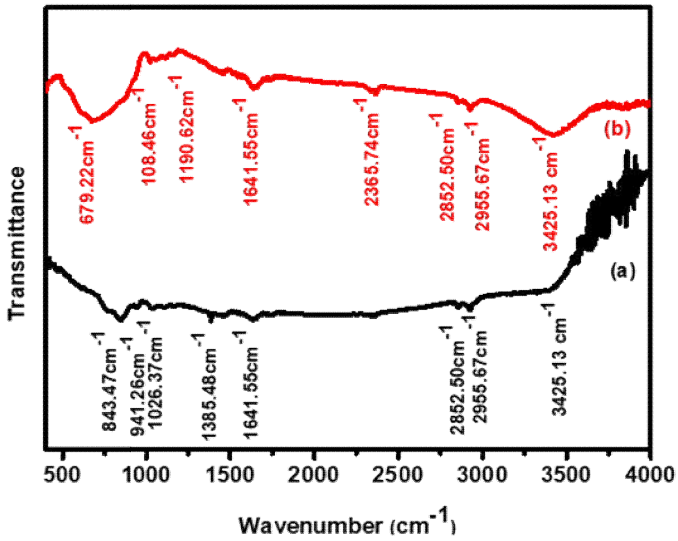

Figure 6. FT-IR spectra of (a) as prepared and (b) annealed LAMOX film.

4. Conclusion

LAMOX thin films shows monoclinic and cubic crystal structures for pre-annealed and annealed films respectively. The porous grain morphology was confirmed from FESEM micrographs. The elemental composition in films is confirmed from EDAX and it approximately in good stoichiometric proportion. FT-IR spectra confirm the absence of surface impurities and assure the formation of pure phase LAMOX. This nature of LAMOX provides excellent electrolytic properties useful for the ion conduction in SOFC.

Acknowledgments

The work is supported by department of physics Dong Hwa University, Hualien, Taiwan.

References

[1] B. C. H. Steele and A. Heinzel, "Materials for fuel cell technologies", Nature, vol. 414, no. 2, (2001), pp. 224-231.

[2] Gregor Hoogers, Fuel cell Handbook, CRC Press (2002).

[3] B. C. H. Steele, "Material science and engineering: The enabling technology for the commercialisation of fuel cell systems", Journal of Materials Science, vol. 36, no. (2001), pp.1053–1068.

[4] B. B. Patil, A. D. Pawar, D. B. Bhosale, J. S. Ghodake, J. B. Thorat & T. J. Shinde, "Effect of La^{3+} substitution on structural and magnetic parameters of Ni–Cu–Zn nano-ferrites", Journal of Nanostructure in Chemistry, vol. 9, no. 1, (2019), pp. 119-128.

[5] B. B. Patil, A. D. Pawar, S. S. Barate, J. S. Ghodake, J. B. Thorat, T. J. Shinde, "Impact of La^{3+} substitution on electrical, magnetic, dielectric and optical properties of $Ni_{0.7}Cu_{0.1}Zn_{0.2}La_xFe_{2-x}O_4$ ($0 < x < 0.035$) system", Journal of Rare Earths, (2022) in press

[6] M. Han, X. Tang, H. Yin, S. Peng, "Fabrication, microstructure and properties of a YSZ electrolyte for SOFCs", Journal of Power Sources, vol. 165, no. 2, (2007), pp. 757-763.

[7] Philippe Lacorre, François Goutenoire, Odile Bohnke, Richard Retoux & Yvon Laligant, "Designing fast oxide-ion conductors based on $La_2Mo_2O_9$", Nature, vol. 404, (2000) pp. 856–858.

[8] P. Lacorre, "The LPS concept, a new way to look at anionic conductors", Solid State Sciences, vol. 2, no. 8, (2000), pp. 755-758.

[9] I. R. Evans, J. A. K. Howard, J. S.O. Evans, "The Crystal Structure of α-$La_2Mo_2O_9$ and the Structural Origin of the Oxide Ion Migration Pathway", Chem. Mater., vol. 17, no. 16, (2005), pp. 4074–4077.

[10] F. Goutenoire, O. Isnard, E. Suard, O. Bohnke, Y. Laligant, R. Retoux and Ph. Lacorre, "Structural and transport characteristics of the LAMOX family of fast oxide-ion conductors, based on lanthanum molybdenum oxide $La_2Mo_2O_9$", J. Mater. Chem., vol. 11, (2001), pp.119-124.

[11] B. C. H. Steel, "Oxygen ion conductors and their technological applications", Materials Science and Engineering: B, vol. 13, no. 2, (1992), pp. 79-87.

[12] J. C. Boivin and G. Mairesse, "Recent Material Developments in Fast Oxide Ion Conductors", Chem. Mater., vol.10, no. 10, (1998), pp. 2870–2888.

[13] N. Q. Minh, "Ceramic Fuel Cells", J. Am. Ceram. Soc., vol. 76, no. 3, (1993), pp. 563-588.

[14] J. B. Goodenough, "oxide ion electrolyte", Annual Review Mater. Res., vol. 33 (2003), pp. 91-128.

[15] S. Diethelm and J. Van Herle, "Oxygen transport through dense $La_{0.6}Sr_{0.4}Fe_{0.8}Co_{0.2}O_{3-\delta}$ perovskite-type permeation membranes", Journal of the European Ceramic Society, vol. 24, no. 6, (2006), pp. 1319-1323.

[16] Samuel Georges, Renata Ayres Rocha, and Elisabeth Djurado, "Microstructure Related Conductivity in $La_2Mo_2O_9$ Ceramics", J. Phys. Chem. C, vol. 112, no. 9, (2008), 112, 3194-3202.

[17] F. Goutenoire, O. Isnard, R. Retoux, Ph. Lacorre, "Crystal Structure of $La_2Mo_2O_9$, a New Fast Oxide−Ion Conductor", Chemistry Material, vol. 12, no. 9, (2000), pp. 2575-2580.

[18] M. Ali (Basu), B. Wani, and S. Bharadwaj, "Phase transition in LAMOX type compounds", Journal of Thermal Analysis and Calorimetry, vol. 96, no. 2, (2009) 463-468.

[19] J. Vega-Castillo, L. Mognia, G. Corbel, P. Lacorre, A. Caneiro, "On the thermodynamic stability of La2Mo2O9−δ oxide-ion conductor", International Journal of Hydrogen Energy, vol. 35, no. 11, (2010), 5890-5894.

[20] I. P. Marozau, D. Marrero-López, A. L Shaula, V. V. Khartona, E.V. Tsipis, PNúñez, J. R Frade, "Ionic and electronic transport in stabilized β-La2Mo2O9 electrolytes", Electrochimica Acta, vol. 49, no. 21, (2004), pp. 3517-3524.

[21] A. Khaled, J. Pireaux and S. Khelili, "Synthesis and Characterization of Ca and Ba Doped LAMOX Materials and Surface Study by X-ray Photoelectron Spectroscopy", Acta Chim. Slov. vol. 59, (2012), pp. 766-778.

[22] Xian-Zhu Fu, Jing-LiLuo Alan R.Sanger, Nancy LuoKarl T.Chuang, "Y-doped $BaCeO_{3-\delta}$ nano powders as proton-conducting electrolyte materials for ethane fuel cells to co-generate ethylene and electricity", J. Power Sources, vol. 195, no. 9, (2010), 2659-2663.

[23] N Dharuman, M Arulmozhi, Mukiri Soban Babu, L John Berchmans & Gosipathala Sreedhar, "Investigations on oxidation, hot corrosion and thermal gradient performance of low k-$La_2Mo_2O_9$ thermal barrier coating", Bulletin of Materials Science, vol. 44, no. 8, (2021), pp. 1-13.

[24] Xia Tian, Li Jia-Yan, Luo Xin, Li Qin, Meng Jian, Cao Xue-Qiang, "Electrical Properties and Dilatometric Measurements of $La_2Mo_2O_9$ under Low Oxygen Partial Pressure", Chinees journal of chemistry, vol. 23, no.6, (2005), pp. 703-708.

[25] R. J. Sayyad, S. R. Gadale, "Synthesis, Characterization And Photocatalytic Activity Of Nanocrystalline Lanthanum Doped Molybdenum Oxide", Journal of Advanced Scientific Research, vol. 13, no. 1, (2022), pp. 153-161.

[26] R. A. Rocha and E. N. S. Muccillo, "Synthesis and Thermal Decomposition of a Polymeric Precursor of the $La_2Mo_2O_9$ Compound", vol. 15, no. 22, Chem. Mater. 2003, pp. 4268–4272.

[27] T. Matsumoto, K. Sunada, T. Nagai, T. Isobe, S. Matsushita, H. Ishiguro, A. Nakajima, "Preparation of hydrophobic $La_2Mo_2O_9$ ceramics with antibacterial and antiviral properties",

journal of Hazardous Materials, vol. 378, (2019), pp. 120610.

[28] Q. Zheng Zhang, Y. Ting Wang, X. Cheng, X. Liu, Y. Qin Zhang, J. Jun Zhou, J Cheng, "Synthesis of Spherical $La_2Mo_2O_9$ Nanoparticles Using Sol-Gel Process" Advanced Materials Research, vol. 933, (2014), pp. 8-11.

[29] A. Subramania, T. Saradha, S. Muzhumathi, "Synthesis and characterization of nanocrystalline $La_2Mo_2O_9$ fast oxide-ion conductor by an in-situ polymerization method", Materials Research Bulletin, vol. 43, no. 5, (2008), pp. 1153-1159.